ARTICLES

Snowball Earth prevention by dissolved organic carbon remineralization

W. Richard Peltier[1], Yonggang Liu[1] & John W. Crowley[1]

The 'snowball Earth' hypothesis posits the occurrence of a sequence of glaciations in the Earth's history sufficiently deep that photosynthetic activity was essentially arrested. Because the time interval during which these events are believed to have occurred immediately preceded the Cambrian explosion of life, the issue as to whether such snowball states actually developed has important implications for our understanding of evolutionary biology. Here we couple an explicit model of the Neoproterozoic carbon cycle to a model of the physical climate system. We show that the drawdown of atmospheric oxygen into the ocean, as surface temperatures decline, operates so as to increase the rate of remineralization of a massive pool of dissolved organic carbon. This leads directly to an increase of atmospheric carbon dioxide, enhanced greenhouse warming of the surface of the Earth, and the prevention of a snowball state.

During the Neoproterozoic era of the Earth's history, the carbon cycle exhibited a sequence of oscillation-like variations that included decreases of $\delta^{13}C$ to levels that have been interpreted to imply the occurrence of intense snowball glaciations[1] during which photosynthetic activity essentially ceased[2–4]. Such events would have strongly affected the evolution of eukaryotic life and this has led to suggestions that this extreme interpretation of the observed variability in the carbon cycle could be unwarranted[5,6]. We have developed a coupled model of the co-evolution of Neoproterozoic climate and the carbon cycle that provides an alternative interpretation to the 'hard snowball' hypothesis of the origin of the observed $\delta^{13}C$ variations. This model links a previously developed model of the Neoproterozoic physical climate system[7,8] to a recently developed model of the carbon cycle[9] for the same time interval. The coupled model is shown to support a limit cycle oscillation in which the temperature dependence of the solubility of oxygen in sea water controls the rate of remineralization of organic carbon such that the level of atmospheric CO_2 is prevented from becoming sufficiently low to allow a hard snowball state to occur. The model also satisfies the timescale and continental ice volume constraints that have been inferred to characterize these glaciation events, as well as the magnitude of the carbon cycle excursions when an appropriate biogeochemical dependence of photosynthetic carbon isotopic fractionation is assumed.

The sequence of intense glaciations that occurred during the Cryogenian period of the Neoproterozoic era—a period that began approximately 850 million years (Myr) ago and which ended approximately 635 Myr ago with the onset of the Ediacaran period—is currently an intense focus of interdisciplinary activity[10]. Evolutionary biologists and palaeontologists[11,12] are interested in this era because it preceded the Cambrian explosion of life, during which eukaryotic biological diversity proliferated. Climate dynamicists[13–18] have been attracted by the challenge posed by the appearance in the geological record of continental-scale glaciation that is suggested to have reached sea level in equatorial latitudes at some locations. Sedimentologists[19–21] and geochronologists[22] have worked on the global-scale correlation of glacial units across the present-day continents, during a time of intense tectonic activity involving the break-up of the supercontinent of Rodinia. However, many important

questions are still unresolved. In particular, how many glaciations actually occurred during the Cryogenian period is currently uncertain. Figure 1, a revised and extended version of previously published sketches[23–25] of the evolution of $\delta^{13}C$ over the most recent billion years of the Earth's history, illustrates the connection in time between this measure of climate variability, major tectonic events, and periods of intense glaciation.

The nature of Cryogenian glacial episodes

Although some recent work has championed the notion that only three major glaciations occurred during this period[23]—the Sturtian glaciation at 723^{+16}_{-10} Myr ago, the Marinoan glaciation between 659 and 637 Myr ago, and the Gaskiers glaciation at approximately 582 Myr ago—there remain significant issues concerning the synchroneity of these events as inferred on the basis of the stratigraphic record from different continents. The chronological control upon the Sturtian glaciation, in particular, now suggests that it consisted of at least two distinct glacial episodes[22]. Evidence from the Huqf Supergroup of Oman has recently been interpreted to imply that no hard snowball glaciation event could have occurred[19–21]. Similarly, the duration of individual glacial episodes remains unknown (although it has been speculated to be between 4 and 30 million years[4]), as is the answer to the question of whether each of the glacial episodes consisted of a single ice advance and retreat or of multiple such events.

A previously proposed model of Neoproterozoic climate suggested the plausibility of a "slushball" solution in which a significant region of open water could have persisted at the Equator during each of these events. This model has been criticized[26] on the basis of the claim that it could not explain the inferred requirement of the geological record for the occurrence of episodes of glaciation that lasted at least 4 Myr. This is the point of departure for the analyses described in this paper. Our target has been the question posed by the carbon isotopic variability depicted qualitatively in Fig. 1. Whereas subsequent to the Neoproterozoic era the carbon cycle appears to have been operating in a quasi-equilibrium mode[9], during the Neoproterozoic it appears to have been operating in an out-of-equilibrium mode that is peculiar to this interval of the Earth's history. This mode of behaviour was recently suggested[9] to have arisen as a consequence of a significant

---

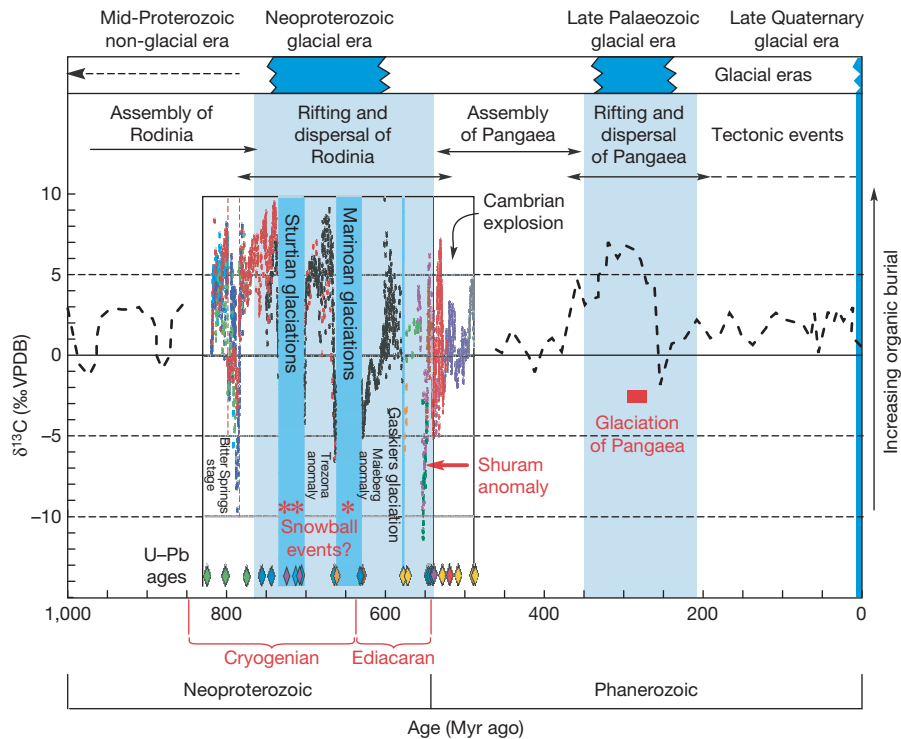[1]Department of Physics, University of Toronto, Toronto, Ontario M5S 1A7, Canada.

Figure 1 | The history of $\delta^{13}C_{inorg}$ variations over the past billion years as measured in sequences of carbonate rocks on land. This quantity provides an indirect measure of photosynthetic activity. High values correspond to times of high rates of burial of organic matter, a consequence of the fact that isotopically light carbon (^{12}C) is preferentially partitioned into organic matter by photosynthesis. Burial of this matter leaves behind an ocean that is isotopically heavier than average, from which the carbonates are precipitated. The Neoproterozoic era was clearly characterized by extreme variability in $\delta^{13}C_{inorg}$. The largest-amplitude negative anomaly that is inferred to have existed during the Neoproterozoic is the Shuram anomaly[35], which is taken to correspond to the major oxidation event that eliminated the condition

required for out-of-equilibrium behaviour of the carbon cycle, namely the extreme imbalance between the masses of the inorganic and organic reservoirs. This figure is a modified version of those originally produced by Kaufman[2] (Fig. 2), Eyles and Januszczak[25] (Fig. 9) and Halverson *et al.*[23] (observational data used with permission). The data presented through the Cryogenian interval are based upon the recently compiled composite record of ref. 23 and are reproduced here with permission. The diamond-shaped symbols represent the times for which high-quality radiometric age determinations (based on the U–Pb dating of detrital zircons) are available to provide chronological control on the sequence of Neoproterozoic events. VPDB, Vienna Pee-Dee belemnite standard.

imbalance between the mass of carbon stored in the Neoproterozoic ocean in the organic and inorganic forms. Atmospheric oxygen could have provided an important link between the carbon cycle and climate but no detailed discussion was provided[9]. The purpose of the analyses reported here is to elaborate a plausible linkage and to investigate the extent to which this may shed light upon the state of the Earth's physical climate system during this critical period for biological evolution.

Coupled carbon cycle–climate evolution

A schematic of the model we have developed for this purpose is shown in Fig. 2, consisting of three primary elements: a model of the carbon cycle[9], a model of the physical climate system (consisting of surface energy balance and sea-ice components[8]), and a detailed model of continental-scale glaciation (the University of Toronto Glacial Systems Model; ref. 27). The mathematical details of the carbon cycle component of the complete coupled model, which involve a significant extension of the model of ref. 9, are described in the Supplementary Information). To link these models we explicitly incorporated a dependence of the remineralization flux J_{21} (Fig. 2), through which organic carbon is converted to inorganic carbon, upon the (temperature-dependent) solubility of oxygen in sea water:

$$J_{21} = J_{21_e}[1 - F_{21}(T - T_e)] \qquad (1)$$

In this expression, T is the mean surface temperature of the planet determined by the physical climate model and T_e is the equilibrium temperature at which the remineralization flux J_{21} equals its equilibrium value. For a discussion of the physical significance of the

control parameter F_{21}, please see Methods. A primary assumption of the present version of the model is that the variations in
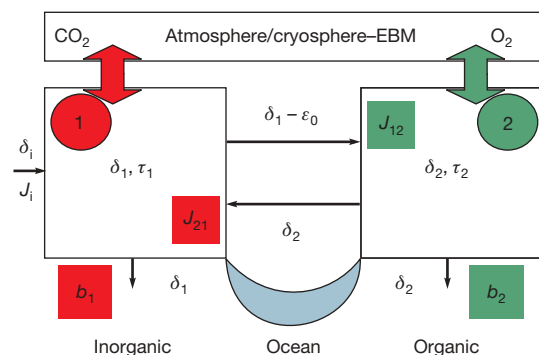

Figure 2 | Diagram of our carbon-cycle-coupled climate model. Its primary component consists of the box model of the carbon cycle of Rothman *et al.*[9], which is coupled to both an energy balance model of the atmosphere (EBM) and the University of Toronto Glacial Systems Model of continental-scale ice-sheet evolution. The variables $\delta_{1,2}$ and $\tau_{1,2}$ are the isotopic compositions and residence times for the inorganic and organic carbon reservoirs, respectively. δ_i is the input into the inorganic reservoir from, for example, volcanic outgassing (of flux J_i) and ε_0 is the isotopic fractionation that occurs in photosynthesis during which inorganic carbon is converted into organic carbon. Fluxes into and out of the two reservoirs are represented by the arrows. Output from the two reservoirs occurs directly by burial (associated with fluxes $b_{1,2}$) as well as by exchanges between them. Crucial to the success of our coupled model of carbon-cycle-climate evolution are the fluxes of O_2 and CO_2 between the atmosphere and ocean components of the model.

atmospheric oxygen that accompany system evolution will have no significant impact upon system dynamics.

The reason that the temperature dependence of the remineralization flux has important implications for the surface climate regime is connected to the fact that as the climate cools and the rate of conversion of organic carbon to inorganic carbon increases, the partial pressure of carbon dioxide in the atmosphere also increases, according to the relation:

$$\frac{p_{CO_2}(t)}{p_{CO_2,\,e}} = \left[\frac{M_1(t)}{M_{1_e}}\right]^X \tag{2}$$

in which $p_{CO_2,\,e} = 300$ p.p.m.v. is the equilibrium concentration of atmospheric carbon dioxide at temperature T_e, M_1 is the mass of inorganic carbon in the ocean and M_{1_e} is the equilibrium mass. It has been suggested[28] that the parameter X in equation (2) should be equal to 2 in Phanerozoic circumstances in which the climate is not changing too quickly. It is unclear whether the partition of carbon dioxide between the ocean and the atmosphere during the rapidly changing Neoproterozoic should obey this relationship, so we consider X to be a parameter of the model. As the level of atmospheric CO_2 increases in response to increasing $M_1(t)$, the surface of the planet will be increasingly heated by the increasing infrared flux of energy d_{rad} (in units of W m^{-2}) that is due to 'greenhouse' warming[29,30]:

$$d_{rad} = 6.0 \ln\left(\frac{p_{CO_2}(t)}{p_{CO_2,\,e}}\right) \tag{3}$$

The sequence of relationships (1) to (3) together describe a negative feedback process whereby the carbon cycle reacts to a tendency of the planet to cool by enhancing the atmospheric concentration of carbon dioxide and thus inhibiting the cooling. During warming the same feedback operates so as to inhibit this tendency as well. The new coupled model of carbon cycle–climate evolution that we have developed for the Neoproterozoic is strongly controlled by this feedback process.

Cyclic glaciation due to carbon cycle coupling

In the absence of explicit coupling to the carbon cycle, the ice-sheet-coupled energy-balance model of the process of global glaciation produces steady-state solutions for the mean surface temperature that are a strong function of the concentration of carbon dioxide in the atmosphere, of the solar constant, and of the spatial distribution of the continents. Although the detailed palaeogeography of the Neoproterozoic varied appreciably during the break-up of Rodinia, there is general agreement that during the Sturtian episode(s) the continental fragments were clustered around the Equator. During the Marinoan episode, however, the equatorial positioning of the main land masses was apparently less pronounced. Here we use the same palaeogeography as was used in a previous analysis[7] of Neoproterozoic surface temperature conditions, one that is more appropriate to the Marinoan glaciation than to the Sturtian(s). For the value of the solar constant we assume a decrease of 6% below the present value, as is appropriate to this stage of the evolution of the Sun.

In the absence of carbon cycle coupling, Fig. 3a shows the steady-state variations of mean surface temperature predicted by the ice-sheet-coupled EBM, as a function of atmospheric carbon dioxide concentration. This model exhibits hysteresis, such that a range of values of the parameter d_{rad}, and thus p_{CO_2}, exists within which at least two different steady states are equally acceptable solutions. Which state is physically realized depends upon the initial conditions of integration from which the solution is approached, as indicated by the arrows on the different branches of the diagram of steady-state solutions. The hysteresis diagram defines a 'hot branch' of solutions as well as an 'oasis branch', the latter being the branch on which the 'slushball' solutions to the problem of Neoproterozoic climate were originally discovered[8]. In this model the hard snowball solution regime also exists, but to reach it requires that $p_{CO_2}(t)$ reaches sufficiently low values. To escape from the hard snowball state in this model requires approximately 0.3 bar of atmospheric carbon dioxide if the sea-ice albedo is assumed to be equal to 0.6 in the hard snowball regime[7]. This is somewhat lower than a more accurate estimate later obtained with a more complex model[31]. Here we investigate how the climate model will behave when coupled to the explicit model of the carbon cycle.

The results delivered by this model in fully coupled synchronous mode are illustrated in Figs 3b–e, for which examples we have assumed $X = 2$ in equation (2). Figure 3b shows several cycles of
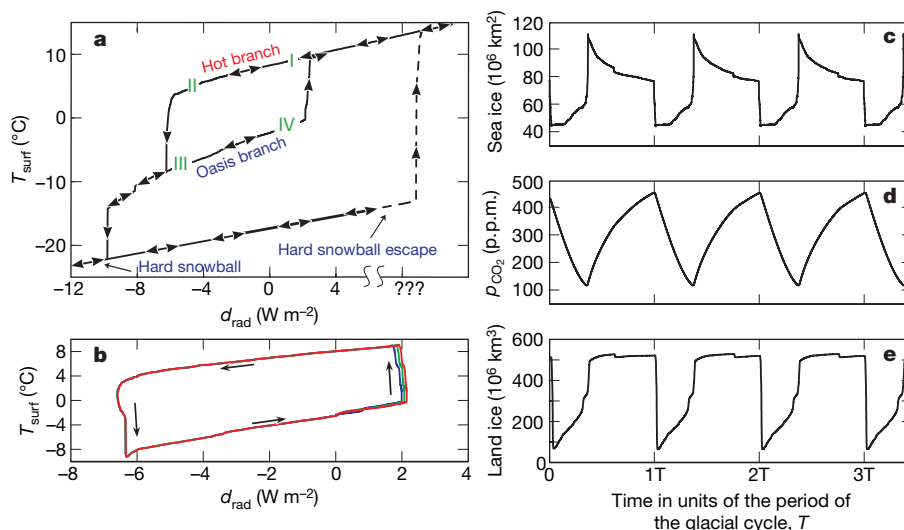

Figure 3 | The cyclic glaciation dynamics of the coupled climate–carbon cycle model. a, The steady-state (equilibrium) solutions of the energy-balance-coupled ice-sheet model are shown as a function of the atmospheric carbon dioxide concentration, represented by the increase or decrease of the infrared flux, d_{rad}, received at the surface. The hysteresis in the model state space is indicated by the multiple equilibria for a wide range of values of the carbon dioxide concentration. **b,** The trajectory of solutions of the coupled climate–carbon cycle model in the space of mean surface temperature versus d_{rad}. surface infrared forcing. The solution simply cycles the hysteresis loop of the steady-state solutions when the impact of the temperature dependence of the solubility of oxygen upon the remineralization flux is introduced into the dynamical system. **c–e,** Time series for sea-ice area, atmospheric carbon dioxide concentration and land-ice volume are shown, respectively, for several circuits of the hysteresis loop. The scale of the x axis depends on the control parameter F_{21}, as demonstrated in Fig. 4.

the 'orbit' of the solution in the plane of mean surface temperature versus d_{rad}. These results demonstrate that the coupled system evolves in such a way as to continuously cycle the hysteresis loop defined by the set of steady-state solutions. In Figs 3c–e we show time series for sea-ice area, atmospheric CO_2 and continental ice volume respectively, for several circuits of the hysteresis loop. These results demonstrate that system evolution is governed by a limit cycle oscillation (a periodic solution of the nonlinear dynamical system) which would have a period of approximately 4 Myr for $F_{21} = 8 \times 10^{-5}$ and a period of approximately 30 Myr for $F_{21} = 1 \times 10^{-5}$. Detailed analysis (not shown) demonstrates that the onset of the periodic behaviour for $X = 1$ occurs for $F_{21} < F_{21, crit}$, where the critical value is in the range $5 \times 10^{-4} < F_{21, crit} < 6 \times 10^{-4}$. For values less than this, the period of the limit cycle oscillation continues to increase as the value of the control variable decreases. For $X = 2$, the critical value of F_{21} is shifted to the range $3 \times 10^{-4} < F_{21, crit} < 4 \times 10^{-4}$.

Figure 4, based upon analyses for several values of the control parameter, for which time series are shown in Supplementary Fig. 1 (for $X = 1$) and Supplementary Fig. 2 (for $X = 2$), shows that the period of the limit cycle covers the previously inferred range of durations of the Neoproterozoic glacial intervals from 4 to ~30 Myr ago. In the limit $F_{21} \to 0$, the previous model[9] is recovered and the system exhibits no dynamics, as physical climate is now uncoupled from the carbon cycle. For $F_{21} > F_{21, crit}$, the system exits the limit cycle regime (see Supplementary Fig. 1 for $F_{21} = 6 \times 10^{-4}$) and a new steady-state solution is realized, one for which the mean surface temperature is equal to the value T_e (not shown). We interpret this 'fixed point' to represent the in-equilibrium solution for the carbon cycle that has apparently been characteristic for the Phanerozoic eon that followed the Neoproterozoic with the onset of the Cambrian. The model therefore embodies a potential explanation not only of the apparently out-of-equilibrium behaviour characteristic of the Neoproterozoic, but also of the in-equilibrium behaviour that has thereafter generally been the rule[9]. Supplementary Fig. 3 shows normalized time series for all model fields as a means of illustrating the phase relationships between them.

Eustatic sea level and ice volume variations

Figure 5 shows the distribution of land ice and sea ice over the surface of the Earth that the model delivers at each of the corners (labelled I to IV on Fig. 3a) of the hysteresis loop of steady solutions onto which the solution is entrained in the time-dependent limit cycle regime. This regime is essentially perfectly periodic, so this set of four solutions fully characterizes the extremes of system behaviour. The low-temperature,
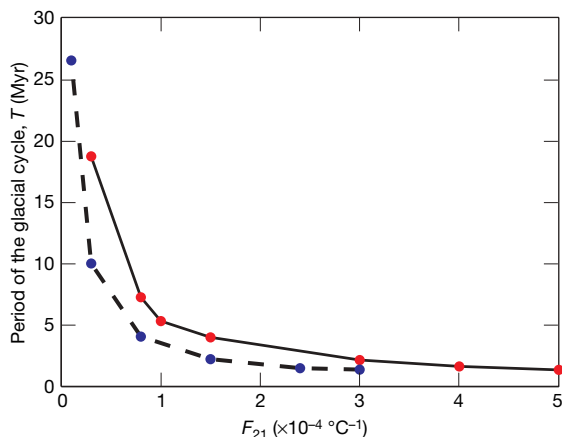
low-carbon dioxide corner of the loop (located at III in Fig. 3a) shows that although most of the continental fragments are covered by a thick veneer of land ice and much of the surface of the ocean is covered by sea ice, there is still a substantial area of the equatorial ocean that consists of open water. This is the 'slushball' regime discovered previously[8]. The maximum volume of land ice that develops during a single glacial cycle is approximately $500 \times 10^6 \, km^3$, as shown on Fig. 3e, which would correspond to a fall of eustatic sea level of approximately 1 km, a result that could be interpreted as consistent with the deep Neoproterozoic canyons that have been investigated on the Australian continent[32,33]. Although much larger, this sea-level depression is still reasonable compared to the sea-level drop of about 120 m that occurred during the Last Glacial Maximum[34], when polar ice sheets covered only a small fraction of the land surface.

We therefore interpret the Cryogenian period as a time during which, in an organic-carbon-rich environment, the mass of organic matter in the Neoproterozoic ocean had reached such a large value relative to the mass of inorganic carbon that out-of-equilibrium behaviour with strong coupling to the physical climate system became possible. In our interpretation, this coupling ceased to be possible after the intense oxidation of the organic reservoir that occurred towards the end of the Ediacaran period and just before the onset of the Cambrian[22]. We interpret this oxidation event as coinciding with the Shuram anomaly shown on Fig. 1[35].

The isotopic variability of inorganic carbon

The model also predicts the time series of $\delta^{13}C(t)$ for the inorganic reservoir, the primary diagnostic that has been taken to require the existence of the hard snowball regime. Escape from this regime is assumed to have been possible only via the build-up of the atmospheric carbon dioxide concentration owing to the presumed slow and continuous action of volcanic degassing while the oceans were entirely covered by sea ice. To make contact with the different isotopic concentrations of organic and inorganic carbon that develop during a single glacial cycle, the isotopic fractionation ε_0 that occurs during photosynthesis (see Fig. 2) must also depend upon ocean biogeochemistry, and thus climate. To predict the evolution of carbon isotopes we may therefore assume:

$$\varepsilon_0 = \varepsilon_e + \beta_{frac, M}(M_1[CO_2(t)] - M_{1_e}) \tag{4}$$

This representation of the isotopic fractionation that occurs during photosynthesis is intended to provide a parameterization of the

Figure 4 | The period of the glacial cycle predicted by the coupled climate–carbon cycle model as a function of the control parameter of the model F_{21}. Results are shown for both $X = 1$ (solid line) and $X = 2$ (dashed line), where X determines how the atmospheric carbon dioxide concentration changes as the mass of inorganic carbon changes relative to the reference values (equation (2)). The predicted period spans the range previously inferred to have been characteristic of Neoproterozoic glacial intervals.
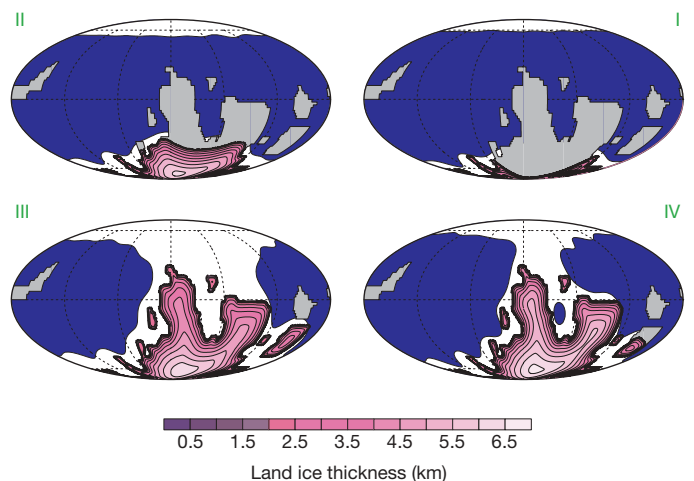
Figure 5 | Examples of the distribution of land ice and sea ice during the glacial cycle. These examples correspond to the climate states occupied by the model at each of the four corners (labelled I to IV) of the hysteresis loop of steady solutions shown on Fig. 3a. Irrespective of the value of the control parameter, in the coupled mode the dynamical system simply continues to cycle the hysteresis loop. Land-ice thickness is contoured in shades of mauve, and sea ice is shown as white.

influence of kinetic isotope effects associated, say, with the enzymatically catalysed carboxylation of ribose bisphosphate (J. M. Hayes, personal communication, 2006). The mass of the inorganic reservoir M_1 is expected to provide a reasonably direct representation of the main control on this catalytic process. This simple parameterization appears to be in acceptable accord with the analyses of ref. 36 as used in the discussion[28] of the dependence of the isotopic difference between organic and inorganic carbon as a function of atmospheric p_{CO_2}. Best fits of the model prediction of the time variation of $\delta^{13}C(t)$ through a typical Neoproterozoic glacial–interglacial cycle based upon the use of equation (4) are obtained with a value of $\beta_{frac,M} \approx 0.00048‰$ per gigaton. This value is not unreasonable given that the species composition of the hypothesized organic-carbon-heavy Neoproterozoic ocean, in which $M_2 \gg M_1$, is largely unknown.

Figure 6a for $X = 2$ shows the model prediction of the evolution of $\delta^{13}C_{inorg}$ as a function of $\varepsilon = \delta_1 - \delta_2$, through a single Neoproterozoic glacial–interglacial cycle, compared with the complete data set from ref. 9, inspection of which demonstrates the good fit that the model is capable of delivering to the data. When the comparison is limited to the interval of time from 738 to 593 Myr ago that contains the Sturtian and Marinoan events (Fig. 6b), however, the fit of the model to the data significantly improves. This demonstrates that the carbon isotopic measurements from the interval containing the hypothesized hard snowball events are well explained by the carbon-cycle-coupled slushball model. As discussed in ref. 9, the slope of the model fit to the data in the $\delta^{13}C_{inorg}$ versus ε plane is unity, which is highly diagnostic of the condition $M_2 \gg M_1$ that is characteristic of the carbon cycle component of the model. Supplementary Fig. 4 shows equivalent results for the case $X = 1$.

Future model developments

Among several further avenues of investigation as we continue to develop this model of the coupled evolution of the carbon cycle and climate during the Neoproterozoic, one we intend to explore concerns the potential of the model as an explicit means of assessing the magnitude of the variations of atmospheric oxygen that would be expected to accompany the glaciation–deglaciation process. Another concerns whether oxidants other than oxygen, such as sulphate, may have an important role to play. Also, how might the drawdown of atmospheric carbon dioxide from the atmosphere due to the weathering of calcium and magnesium silicates be expected to affect our model predictions[16]? Here we neglected this drawdown because of the strong temperature and precipitation dependence that is characteristic of the silicate weathering process, such that low temperature and precipitation and the absence of vascular plants in this period of the Earth's history would have significantly reduced its effect[37–39]. In spite of this and other remaining uncertainties, the new model strongly suggests that those observations that have been assumed to be most diagnostic of hard snowball conditions may not require such an extreme interpretation. In our view it is more likely that it may have been the carbon cycle, not the physical climate system, that was operating in an extreme mode before the onset of the Cambrian explosion of life.

METHODS SUMMARY

Our model consists of three primary components. (1) A global surface energy balance model in spherical geometry with a specified distribution of continents and ocean coupled to a simple thermodynamic model of sea-ice formation. This element of the structure is time-dependent and may be subjected to orbital insolation variations. It also resolves the annual cycle of surface temperature. (2) A detailed model of the growth and evolution of continental ice sheets that occurs in response to variations in the surface temperature and precipitation regimes. In this model, precipitation forcing of the hydrological cycle is prescribed. Furthermore, the glacial isostatic adjustment process that affects the flow of ice over the surface of a continent under the action of the gravitational force is fully incorporated. (3) A two-box model of the ocean carbon cycle that differentiates between organic and inorganic reservoirs. Components (1) and (2) are described in terms of coupled nonlinear partial differential equations whereas the third component is described in terms of coupled nonlinear ordinary differential equations. On the long timescales that are of interest to us we may safely assume the concentration of carbon dioxide to be uniform throughout the atmosphere at all times, because CO_2 is a well-mixed atmospheric trace gas. The three model components are coupled together through the action of an assumed temperature dependence of the remineralization flux that converts organic carbon to its inorganic (CO_2) form. The temperature assumed to control the remineralization flux is taken to be the mean surface temperature of the planet, a temperature that is dominated by the sea-surface temperature of the tropical ocean.

Full Methods and any associated references are available in the online version of the paper at www.nature.com/nature.

1. Kirschvink, J. L. in *The Proterozoic Biosphere: A Multi-Disciplinary Study* (eds Schopf, J. W. & Klein, C.) 51–52 (Cambridge Univ. Press, Cambridge, UK, 1992).
2. Kaufman, A. J. An ice age in the tropics. *Nature* **386**, 227–228 (1997).
3. Hoffman, P. F., Kaufman, A. J., Halverson, G. P. & Schrag, D. P. A Neoproterozoic Snowball Earth. *Science* **281**, 1342–1346 (1998).
4. Hoffman, P. F. & Schrag, D. P. The snowball Earth hypothesis: testing the limits of global change. *Terra Nova* **14**, 129–155 (2002).
5. Runnegar, B. Loophole for snowball Earth. *Nature* **405**, 403–404 (2000).
6. Knoll, A. H. *Life on a Young Planet: The First Three Billion Years of Evolution on Earth* 1–277 (Princeton Univ. Press, Princeton, New Jersey, 2003).
7. Hyde, W. T., Crowley, T. J., Baum, S. K. & Peltier, W. R. Neoproterozoic "Snowball Earth" simulations with a coupled climate/ice-sheet model. *Nature* **405**, 425–429 (2000).
8. Peltier, W. R., Tarasov, L., Vettoretti, G. & Solheim, L. P. in *The Extreme Proterozoic: Geology, Geochemistry and Climate* (eds Jenkins, G. S. *et al.*) Geophys. Monogr. Ser., **146**, 107–124 (AGU Press, Washington DC, 2004).
9. Rothman, D. H., Hayes, J. M. & Summons, R. E. Dynamics of the Neoproterozoic carbon cycle. *Proc. Natl Acad. Sci. USA* **100**, 8124–8129 (2003).
10. Allen, P. A. Snowball Earth on trial. *Eos* **87**, 495 (2006).
11. Moczydlowska, M. Neoproterozoic and Cambrian successions deposited on the east European platform and Cadomian basement area of Poland. *Stud. Geophys. Geodaetica* **39**, 276–285 (1995).
12. Grey, K. & Corkoran, M. Late Neoproterozoic stromatolites in glacigenic successions of the Kimberley region, Western Australia: evidence for a younger Marinoan glaciation. *Precambr. Res.* **92**, 65–87 (1998).
13. Chandler, M. A. & Sohl, L. E. Climate forcings and the initiation of low-latitude ice sheets during the Neoproterozoic Varanger glacial interval. *J. Geophys. Res.* **105**, 20737–20756 (2000).
14. Goodman, J. C. & Pierrehumbert, R. T. Glacial flow of floating marine ice in "Snowball Earth". *J. Geophys. Res.* **108**, doi:10.1029/2002JC001471 (2003).
15. Poulsen, C. J. & Jacob, R. L. Factors that inhibit snowball Earth simulation. *Paleoceanography* **19**, doi:10.1029/2004PA001056 (2004).
16. Donnadieu, Y., Goddéris, Y., Ramstein, G., Nédélec, A. & Meert, J. A. "Snowball Earth" triggered by continental breakup through changes in runoff. *Nature* **428**, 303–306 (2004).
17. Pollard, D. & Kasting, J. F. Snowball Earth: a thin ice solution with flowing sea glaciers. *J. Geophys. Res.* **110**, doi:10.1029/2004JC002525 (2005).
18. Pierrehumbert, R. T. Climate dynamics of a hard snowball Earth. *J. Geophys. Res.* **110**, doi:10.1029/2004JD0005162 (2005).
19. Leather, J., Allen, P. A., Brasier, M. D. & Cozzi, A. Neoproterozoic snowball Earth under scrutiny: Evidence from the Fiq glaciation of Oman. *Geology* **30**, 891–894 (2002).
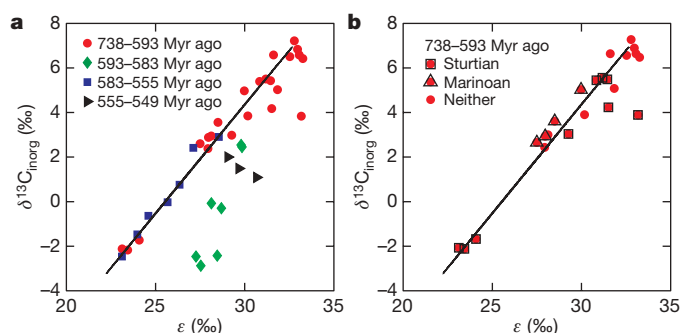
Figure 6 | Model predictions of $\delta^{13}C_{inorg}(t)$ as a function of $\varepsilon(t)$ through a single glacial cycle. These examples for the case $X = 2$ are compared with observations of contemporaneous samples of the isotopic ratios of organic and inorganic carbon at a large number of times through the Neoproterozoic. **a**, Comparison of all of the available data from Rothman *et al.*[9]. **b**, The data derived from 738–593 Myr ago are shown separately and the data points from the Sturtian and Marinoan intervals are singled out.

20. Le Guerroué, E., Allen, P. A. & Cozzi, A. Chemostratigraphic and sedimentological framework of the largest negative carbon isotopic excursion in Earth history: The Neoproterozoic Shuram formation (Nafun Group, Oman). *Precambr. Res.* **146,** 68–92 (2006).

21. Allen, P. A., Leather, J. & Brasier, M. D. The Neoproterozoic Fiq glaciation and its aftermath: Huqf Supergroup of Oman. *Basin Res.* **16,** 507–534 (2004).

22. Condon, D. *et al.* U-Pb ages from the Neoproterozoic Doushantuo formation, China. *Science* **308,** 95–98 (2005).

23. Halverson, G. P., Hoffman, P. F., Schrag, D. P., Maloof, A. C. & Rice, A. H. N. Towards a Neoproterozoic composite carbon cycle isotopic record. *Geol. Soc. Am. Bull.* **117,** 1181–1207 (2005).

24. Hoffman, P. F. & Schrag, D. P. Snowball Earth. *Sci. Am.* **282,** 68–75 (2000).

25. Eyles, N. & Januszczak, N. ''Zipper-Rift'': A tectonic model for Neoproterozoic glaciations during the breakup of Rodinia after 750 Ma. *Earth Sci. Rev.* **65,** 1–73 (2004).

26. Schrag, D. P. & Hoffman, P. F. Life, geology, and snowball Earth. *Nature* **9,** 306 (2001).

27. Tarasov, L. & Peltier, W. R. Arctic freshwater forcing of the Younger-Dryas cold reversal. *Nature* **435,** 662–665 (2005).

28. Kump, L. R. & Arthur, M. A. Interpreting carbon-isotope excursions: carbonates and organic matter. *Chem. Geol.* **161,** 181–198 (1999).

29. Ramanathan, V., Lian, M. S. & Cess, R. D. Increasing atmospheric CO_2: zonal and seasonal estimates of the effect on the radiation energy balance and surface temperature. *J. Geophys. Res.* **84,** 4949–4958 (1979).

30. Marshall, H. G., Walker, J. C. G. & Kuhn, W. R. Long-term climate change and the geochemical cycle of carbon. *J. Geophys. Res.* **93,** 791–801 (1988).

31. Pierrehumbert, R. T. High levels of atmospheric carbon dioxide necessary for the termination of global glaciation. *Nature* **429,** 646–649 (2004).

32. Christie-Blick, N., von der Borch, C. C. & Dibona, P. A. Working hypotheses for the origin of the Wonoka canyons (Neoproterozoic), South Australia. *Am. J. Sci. A* **290,** 295–332 (1990).

33. Christie-Blick, N., Williams, G. E. & Gostin, V. A. Discussion on mantle plume uplift in the sedimentary record: Origin of kilometre-deep canyons within late Neoproterozoic successions, South Australia. *J. Geol. Soc.* **158,** 573–576 (2001).

34. Peltier, W. R. & Fairbanks, R. G. Global glacial ice volume and Last Glacial Maximum duration from an extended Barbados sea level record. *Quat. Sci. Rev.* **25,** 3322–3337 (2006).

35. Fike, D. A., Grotzinger, J. P., Pratt, L. M. & Summons, R. E. Oxidation of the Ediacaran ocean. *Nature* **444,** 744–747 (2006).

36. Bidigare, R. R. *et al.* Consistent fractionation of ^{13}C in nature and in the laboratory: growth-rate effects in some haptophyte algae. *Glob. Biogeochem. Cycles* **11,** 279–292 (1997).

37. Walker, J. C. G., Hays, P. B. & Kasting, J. F. A negative feedback mechanism for the long term stabilization of earth's surface temperature. *J. Geophys. Res.* **86,** 9776–9782 (1981).

38. Berner, R. A., Lasaga, A. C. & Garrels, R. M. The carbonate-silicate geochemical cycle and its effect on atmospheric carbon dioxide over the past 100 million years. *Am. J. Sci.* **283,** 641–683 (1983).

39. Berner, R. A. *The Phanerozoic Carbon Cycle: CO$_2$ and O$_2$* 1–150 (Oxford Univ. Press, Oxford, UK, 2004).

METHODS

By far the most important aspect of the coupled carbon cycle–climate model that we have developed concerns the feedback between temperature and the rate at which organic carbon is remineralized to produce inorganic carbon, as expressed in equation (1). This relationship is supported by the well-known dependence, through Henry's law of classical thermodynamics, of the solubility of a gas in a liquid upon the temperature of the liquid. Garcia *et al.*[40] provide detailed information on the basis of which we justify a linear parameterization of the solubility of oxygen in sea water:

$$O_{2,\,sol} = O_{2,\,sol_e} - A(T - T_e) \tag{5}$$

This dependence is introduced into the carbon cycle model by assuming that the remineralization flux J_{21} is itself linearly dependent upon the deviation of the solubility of oxygen away from its value at an equilibrium temperature T_e. An appropriate modification of the equilibrium flux J_{21_e} that incorporates this dependence (see Supplementary Information) is:

$$J_{21} = J_{21_e} \left\{ 1 + B \left(\frac{O_{2,\,sol} - O_{2,\,sol_e}}{O_{2,\,sol_e}} \right) \right\} \tag{6}$$

Incorporation of equation (5) into equation (6) then gives equation (1) in the main text.

The primary control parameter in the new coupled carbon cycle–climate model is therefore the parameter F_{21}, which has the dimensions of inverse temperature:

$$F_{21} = \frac{AB}{O_{2,\,sol_e}} \tag{7}$$

In the low-temperature vicinity of $1\,^{\circ}C$, $A \approx 8\,\mu mol\,kg^{-1}\,^{\circ}C^{-1}$ (ref. 40) and $O_{2,\,sol} \approx 400\,\mu mol\,kg^{-1}$ (ref. 40). Thus $F_{21} \approx 3 \times 10^{-4}\,^{\circ}C^{-1}$ for $B = 1.5 \times 10^{-2}$ (the importance of this value of F_{21} is discussed in the main text). The strength of the dependence of the remineralization flux upon oxygen solubility that is determined by the parameter B is clearly affected by ocean dynamics, including the strength of the overturning circulation that operates under glacial conditions. Although some model experiments have been performed[8,41] in an attempt to estimate this strength, and it is generally agreed that the thermohaline circulation will act in such a way as to inhibit descent into the hard snowball state, thermohaline circulation behaviour during the Neoproterozoic must be considered ill-constrained at present. This requires that a range of values for the parameter F_{21} be considered. Additional inhibition to snowball Earth formation in the actual climate system may derive from the action of the wind-driven circulation[15] and the detailed characteristics related to sea-ice formation in the tropics[14,15] where incoming solar radiation is especially intense. Such additional processes have been fully incorporated in a recently published simulation[8] of Neoproterozoic climate that has been preformed using the NCAR CSM 1.4 model.

The 'two box model' of the carbon cycle that is assumed to respond to climate variability in the way described by the above relationships is coupled to a global energy balance model (EBM) that is itself coupled to a thermodynamic sea-ice module and a detailed model of continental-scale glaciation. The global EBM is based upon that of North *et al.*[42] as modified by Deblonde *et al.*[43] to include a sea-ice component. Because carbon dioxide is a well-mixed trace gas, when an increase of the remineralization flux occurs as a consequence of decreasing temperature and the resulting increase in carbon dioxide dissolved in the ocean is partly partitioned into the atmosphere, there is no need to consider atmospheric variations in the spatial distribution of this greenhouse gas.

The model of continental-scale glaciation is based upon the use of the standard Glen flow law for the rheology and the shallow-ice approximation for the dynamics. Because the topography of the Neoproterozoic continents is unknown, the ice cover on the individual continental fragments is assumed to develop on continental masses with a fixed initial freeboard of 400 m. As ice flows from the land to sea under the action of the gravitational force, calving is assumed to act so as to eliminate ice beyond the continental termini. Processes such as fast flow which are strongly conditioned by basal hydrology and sediment deformation are eliminated from the model we employed. The isostatic adjustment process that acts to modify the surface elevation of the ice sheet and thus affects the surface mass balance is incorporated by assuming the process to act in a simple damped return-to-equilibrium fashion with an assumed relaxation time of 4,000 years, in acceptable accord with that appropriate for the Earth's present-day radial viscoelastic structure[44]. This is expected to be an excellent approximation because, although the rheology of the planetary interior is strongly temperature-dependent, the temperature of the interior has not changed significantly since Neoproterozoic time[45].

The climate forcing that is assumed to drive the advances and retreats of both continental ice sheets and sea-ice cover is obtained from the surface temperature field delivered by the EBM, assuming an annually averaged precipitation rate of $\sim 0.7\,m\,yr^{-1}$, which is appropriately diminished owing to the action of the elevation desert effect, which acts so as to reduce the precipitation rate in regions of high topographic relief such as for continents covered by substantial thicknesses of glacial ice. These assumptions are the same as those previously employed in the application of this model to the climate of the Neoproterozoic[7]. The physical climate component of the carbon-cycle-coupled model has been thoroughly exercised in a number of recent analyses of climate variations through the Phanerozoic eon[46,47] and in spite of its modest degree of complexity, compared well against expectations based upon the GEOCARB model[48] of past variations in atmospheric carbon dioxide.

40. Garcia, H. E. & Gordon, L. I. Oxygen solubility in sea water: Better fitting equations. *Limnol. Oceanogr.* **37**, 1307–1312 (1992).
41. Poulsen, C. J., Pierrehumbert, R. T. & Jacob, R. L. Impact of ocean dynamics on the simulation of the Neoproterozoic ''snowball Earth''. *Geophys. Res. Lett.* **28**, doi:10.1029/2000GL012058 (2001).
42. North, G. R., Mengel, J. G. & Short, D. A. Simple energy balance model resolving the seasons and continents: application to the astronomical theory of the ice ages. *J. Geophys. Res.* **88**, 6576–6586 (1983).
43. Deblonde, G., Peltier, W. R. & Hyde, W. T. Simulations of continental ice sheet growth over the last glacial-interglacial cycle: experiments with a one level seasonal energy balance model including seasonal ice albedo feedback. *Glob. Planet. Change* **98**, 37–55 (1992).
44. Peltier, W. R. Postglacial variations in the level of the sea: implications for climate dynamics and solid-earth geophysics. *Rev. Geophys.* **36**, 603–689 (1998).
45. Butler, S. L., Peltier, W. R. & Costin, S. O. Numerical models of the earth's thermal history: Effects of inner core solidification and core potassium. *Phys. Earth Planet. Inter.* **152**, 22–42 (2005).
46. Hyde, W. T., Crowley, T. J., Tarasov, L. & Peltier, W. R. The Pangean ice-age: Studies with a coupled climate-ice sheet model. *Clim. Dyn.* **15**, 619–629 (1999).
47. Hyde, W. T., Grossman, E. L., Crowley, T. J., Pollard, D. & Scotese, C. R. Siberian glaciation as a constraint on Permian-Carboniferous CO$_2$ levels. *Geology* **34**, 421–424 (2006).
48. Berner, R. A. GEOCARBSULF: A combined model for Phanerozoic atmospheric O$_2$ and CO$_2$. *Geochim. Cosmochim. Acta* **70**, 5653–5664 (2006).

Snowball Earth prevention by dissolved organic carbon remineralization

W. Richard Peltier, Yonggang Liu & John W. Crowley

Supplementary Information

Since the global ice-sheet coupled energy balance model that is employed in coupled carbon cycle mode in this paper has been well described in the existing literature, only a cursory discussion of its properties will be presented herein. The sole extension to this model beyond that described in Hyde et al.[7] concerns the continental ice-sheet component of this coupled structure. Whereas in Hyde et al.[7] the version of the ice-sheet model (ISM) employed was the isothermal version originally developed by Deblonde et al.[30], the version employed for present purposes is the complete three dimensional thermo-mechanically self consistent version of the model[47]. This version of the ice-sheet model has been subjected to detailed testing in the context of the European EISMINT programme[48] and is at the current state-of-the-art in this area of science. The most recent application of this model has been to a detailed analysis of the history of freshwater runoff from the North American continent during the transition from glacial to interglacial conditions that began following Last Glacial Maximum approximately 21,000 years before present[49]. The EBM to which this ice dynamics model is coupled includes an enhancement of the original North et al.[29] model by the addition of a thermodynamic sea-ice module as discussed in Deblonde et al.[30]. The model also includes a representation of the glacial isostatic adjustment (GIA) process, a process that impacts ice sheet growth and decay through the influence that topography has upon surface mass balance. For the purpose of the analyses described in this paper, GIA effects are incorporated simply as a damped return to equilibrium rather than by employing the more exact theory (e.g. as reviewed in Peltier[31])

The carbon cycle model to which this EBM/ISM is coupled is based upon that presented in Rothman et al.[9]. Since several properties of this model that were not discussed in that paper are important for the purpose of the present application, the mathematical details of the model and the modifications to it that have been made require comment. The original box model is based upon that depicted in Figure 2, which prominently represents the ocean component of the carbon cycle expressed as an interaction between inorganic and organic reservoirs. The ordinary differential equations required to describe this interaction are as follows:

$$\dot{\delta}_1 = \frac{J_i}{M_1}(\delta_i - \delta_1) + \frac{J_{21}}{M_1}(\delta_2 - \delta_1) + \frac{J_{12}}{M_1}\varepsilon_0 \tag{S1}$$

$$\dot{\delta}_2 = \frac{J_{12}}{M_2}(\delta_1 - \varepsilon_0 - \delta_2) \tag{S2}$$

$$\dot{M}_1 = J_i + J_{21} - J_{12} - b_1 \tag{S3}$$

$$\dot{M}_2 = J_{12} - J_{21} - b_2 \tag{S4}$$

In the above equations the subscripted "J" and "b" quantities are mass fluxes that have the dimensions of mass/unit time. The fluxes labeled "b" are burial fluxes that describe the rate of deposition onto the ocean floor of material from the two carbon reservoirs. The subscripted "δ" quantities represent the $\delta^{13}C$ isotopic ratios of reservoirs "1" and "2" and of the isotopic input into reservoir "1" due, for example, to volcanic degassing.

The model of the carbon cycle embodied in equations (S1-S4) has steady state solutions, not catalogued in Rothman et al[9], but which are important in the current context. These steady state solutions may best be described in terms of the following model dependent quantities. If we define by J_1 and J_2 the TOTAL mass fluxes into and out of the inorganic and organic reservoirs respectively, then at equilibrium we must have:

$$J_{1_e} = J_{12_e} + b_{1_e} = J_{i_e} + J_{21_e} \tag{S5}$$
$$J_{2_e} = J_{21_e} + b_{2_e} = J_{12_e} \tag{S6}$$

in which the subscript "e" indicates an equilibrium value. The residence time constants indicated on the box diagram in figure 2 of the paper are defined at steady state to be:

$$\tau_1 = M_{1_e} / J_{1_e} , \tag{S7}$$
$$\tau_2 = M_{2_e} / J_{2_e} . \tag{S8}$$

Additional quantities that are useful in representing the steady state solutions of the Rothman et al.[9] model are the normalized photosynthetic flux, ϕ_{12}, the organic fraction of the total burial flux, f, and the ratio of the residence times μ. These quantities have the following definitions:

$$\phi_{12} = J_{12} / J_1 \tag{S9}$$
$$f = b_2 / (b_1 + b_2) \tag{S10}$$
$$\mu = \tau_1 / \tau_2 \tag{S11}$$

The above defined quantities may be usefully employed to define the steady state solutions.

Detailed algebraic manipulation of the relations that follow from setting the left hand sides of equations (S1)-(S4) to zero (not shown), lead to the following expressions that define the steady states of the carbon cycle model. The critical quantity is the normalized photosynthetic flux ϕ_{12} , the equilibrium value for which can be obtained by substituting from equation (S5) into the definition (S9) to obtain, at equilibrium, that:

$$\phi_{12_e} = J_{12_e} / \left(J_{12_e} + b_{1_e} \right) \tag{S12}$$

In terms of the equilibrium mass of the inorganic carbon reservoir, M_1, the mass of the organic carbon reservoir at equilibrium turns out to be:

$$M_{2_e} = \frac{\phi_{12_e} M_{1_e}}{\mu}, \tag{S13}$$

whereas the equilibrium fluxes connecting the reservoirs to one-another and to the external environment are the following:

$$J_{i_e} = \frac{M_{1_e} \left(1 - \phi_{12_e} \right)}{\tau_1 \left(1 - f \right)} \tag{S14}$$

$$J_{12_e} = \frac{M_{1_e} \phi_{12_e}}{\tau_1} \tag{S15}$$

$$J_{21_e} = \frac{M_{1_e} \phi_{12_e}}{\tau_1} - \left(\frac{f}{1-f} \right) \frac{M_{1_e} \left(1 - \phi_{12_e} \right)}{\tau_1} \tag{S16}$$

It is equation (S16) for the re-mineralization flux that converts organic carbon back to the inorganic form that is critical to the operation of the coupled climate-carbon cycle model presented in this paper. Our assumption in designing this model is that the coupling occurs primarily in an indirect way as a consequence of the strong temperature dependence of the solubility of oxygen in sea water. As it is now well understood that the planetary atmosphere had become rich in oxygen by approximately 2.3 Ga, by the time of the Cryogenian period any occurrence of low surface temperatures that threatened to lead to "hard snowball" surface glaciation would have led to a rapid draw down of oxygen into the ocean as a consequence of Henry's Law of classical thermodynamics. This would have led to a strong increase in the rate of re-mineralization of the organic reservoir and thus to an increase in dissolved inorganic carbon (DIC) and thus, in turn, to an increase of carbon dioxide in the atmosphere and thus strong negative feedback upon the tendency of the surface of the planet to further glaciate. This is the essence of the coupling that links the carbon cycle to the greenhouse gas mediated surface climate regime. Because carbon dioxide is a "well mixed" trace gas, the box model provides an adequate description of the partitioning between the oceanic and atmospheric parts of the whole system inorganic reservoir.

The set of nonlinear ordinary differential equations that replace the original equations (S1)-(S4) of Rothman et al.[9] are obtained by substitution of a surface temperature modulated form of the equilibrium re-mineralization flux J_{21_e} and an appropriate parameterization for the dependence upon climate of the photosynthetic isotopic fractionation ε_0. Otherwise the fluxes that mediate the interactions between the reservoirs and the external environment are taken equal to their equilibrium values. The set of ordinary differential equations that the procedure delivers is the following:

$$\dot{\delta}_1 = \frac{J_{i_e}}{M_1}(\delta_i - \delta_1) + \frac{J_{21_e}}{M_1}(\delta_2 - \delta_1)(1 - F_{21}[T - T_e]) + \frac{J_{12_e}}{M_1}(\varepsilon_e + \beta_{frac}[M_1 - M_{1_e}]) \quad \text{(S17)}$$

$$\dot{\delta}_2 = \frac{J_{12_e}}{M_2}(\delta_1 - \delta_2 - [\varepsilon_e + \beta_{frac}(M_1 - M_{1_e})]) \quad \text{(S18)}$$

$$\dot{M}_1 = -F_{21}J_{21_e}(T - T_e) \quad \text{(S19)}$$

$$\dot{M}_2 = +F_{21}J_{21_e}(T - T_e) \quad \text{(S20)}$$

The model is then completely described by specifying values for the quantities ϕ_{12e}, μ, τ_1, ε_e, δ_i, β_{frac}, T_e and f. The values selected for these parameters for the calculations reported in this paper are essentially identical to those employed in the paper by Rothman et al.[9] and are respectively 0.999, .01, 1000 years, 28 per mil, -6 per mil, variable, 1 degree Celsius, and 0.3. As in the paper by Rothman et al.[9] the selected values for ϕ_{12e} and μ result in an organic reservoir mass that is approximately 100 times the mass of the inorganic reservoir. The initial mass of the inorganic carbon reservoir does not affect the dynamics in any way, but in our calculations has been initialized to the value of 40,000 Giga tons estimated by Kump et al.[50] to be the amount of inorganic carbon present in the modern ocean. The temperature employed for the purpose of coupling the carbon cycle to the model of the physical climate system is taken to be the mean surface temperature for the purpose of the analyses presented in this paper.

Although space has allowed only a single example of the characteristics of solutions to the coupled climate carbon cycle model to be displayed in the main body of the paper, it will be of interest to some readers to see specific examples of the dependence of the time scale of the limit cycle oscillation that the model delivers upon the magnitude of the control parameter F_{21}. This dependence is illustrated in Figures S1 and S2 in which we show a set of simulated time series of continental ice volume for a range of F_{21} values with the value of the parameter "X" (see equ. (2)), that controls the partition of carbon dioxide between the ocean and the atmosphere, set to the value 1 and 2 respectively. A graph of the dependence of the period of the limit cycle oscillation upon this control variable is shown as Figure 4 in the main body of the paper for both $X=1$ and $X=2$. It will be clear on the basis of these results that episodes of glaciation with durations of order a few million years are easily accommodated by the model. Even the period of ~70 million years separating the Sturtian and Marinoan events could be accommodated if this were considered to be the fundamental glacial period since the period diverges to very large values in the limit that $F_{21} \to 0$. This demonstrates that, as a consequence of carbon cycle coupling, "slushball" modes of deep glaciation are easily able to satisfy the claim by Schrag and Hoffman[25] that the geological record requires that episodes of Neoproterozoic glaciation have durations of at least 4 Ma. Figure S3 presents a sequence of amplitude

normalized time series, with the mean removed, for each of the primary field variables of the model. This presentation makes possible an inter-comparison of phase relationships between these characteristics of the model thorugh a number of glacial cycles.

In order to demonstrate that our ability to fit the observed Neoproterozoic variations of the difference between the carbon isotopic ratios of inorganic and organic carbon is not restricted to the case $X=2$, Figure S4 shows the fit for the case $X=1$ for which a different value of the parameter $\beta_{frac} = 0.00028$, rather than the value employed for the case $X=2$ which was 0.00048 and for which results were shown on Figure 6 in the main body of the paper. The simple linear approximation for the dependence of the photosynthetic isotopic fractionation upon the mass of the inorganic carbon reservoir that we are employing for the purpose of the results presented in this paper is very easily accommodated within the more detailed biogeochemical description provided by the model of Kump and Arthur[36]. This simply requires appropriate changes in the constants of their model, constants that were originally derived by fitting to data from the Phanerozoic. Since the Neoproterozoic system differed dramatically from its Phanerozoic counterpart, the requirement for some adjustment of the parameters of their model is required for application to the Neoproterozoic is understandable.

Supplementary References

47. Tarasov, L. & Peltier, W.R. Impact of thermo-mechanical ice sheet coupling on a model of the 100 kyr ice age cycle. J. Geophys. Res. **104**, 9517-9545 (1999).
48. Payne, A.J. et al. Results from the EISMINT model inter-comparison: the effects of thermo-mechanical coupling. J. Glaciology **46**, 227-238 (2000).
49. Tarasov, L. & Peltier, W.R. A calibrated deglacial drainage chronology for the North American continent: Evidence of an Arctic trigger for the Younger-Dryas. Quat. Sci. Rev. **25**, 659-688 (2006).
50. Kump, L.R., Kasting, J.F. & Crane, R.G. The Earth System. Pearson Education Inc. Upper Saddle River, New Jersey (2004), 419pp.
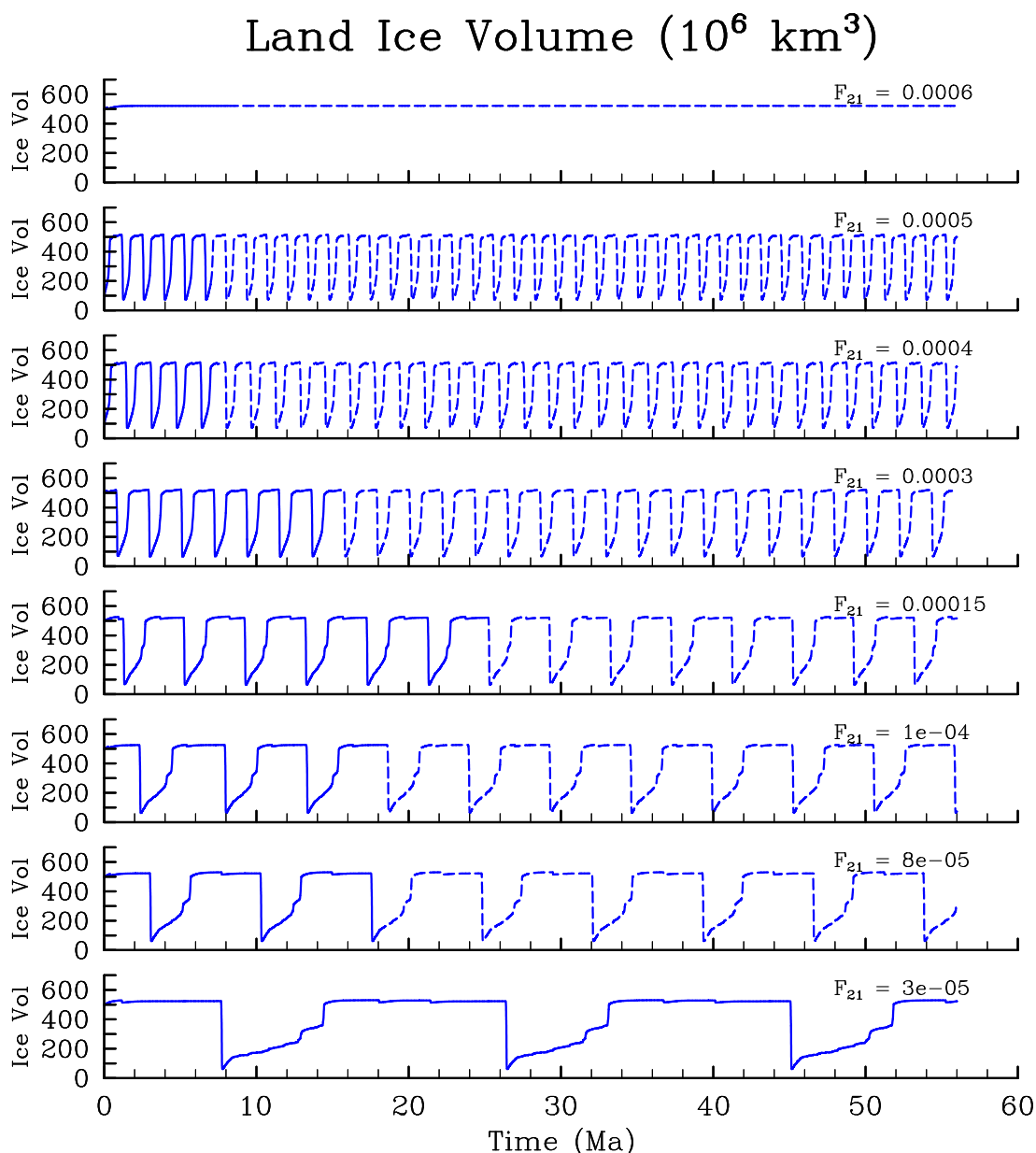
Figure S1 Time series of continental ice volume for a range of F_{21} values, for the model employing linear dependence (namely $X=1$ in equ. (2)) of $p\text{CO}_2$ on the mass of dissolved inorganic carbon. The solid lines are directly from the model calculation, whereas the dashed extensions to each of the time series are extrapolations on the basis of the demonstrated periodicity to enable each of the time series to cover the same range of time.
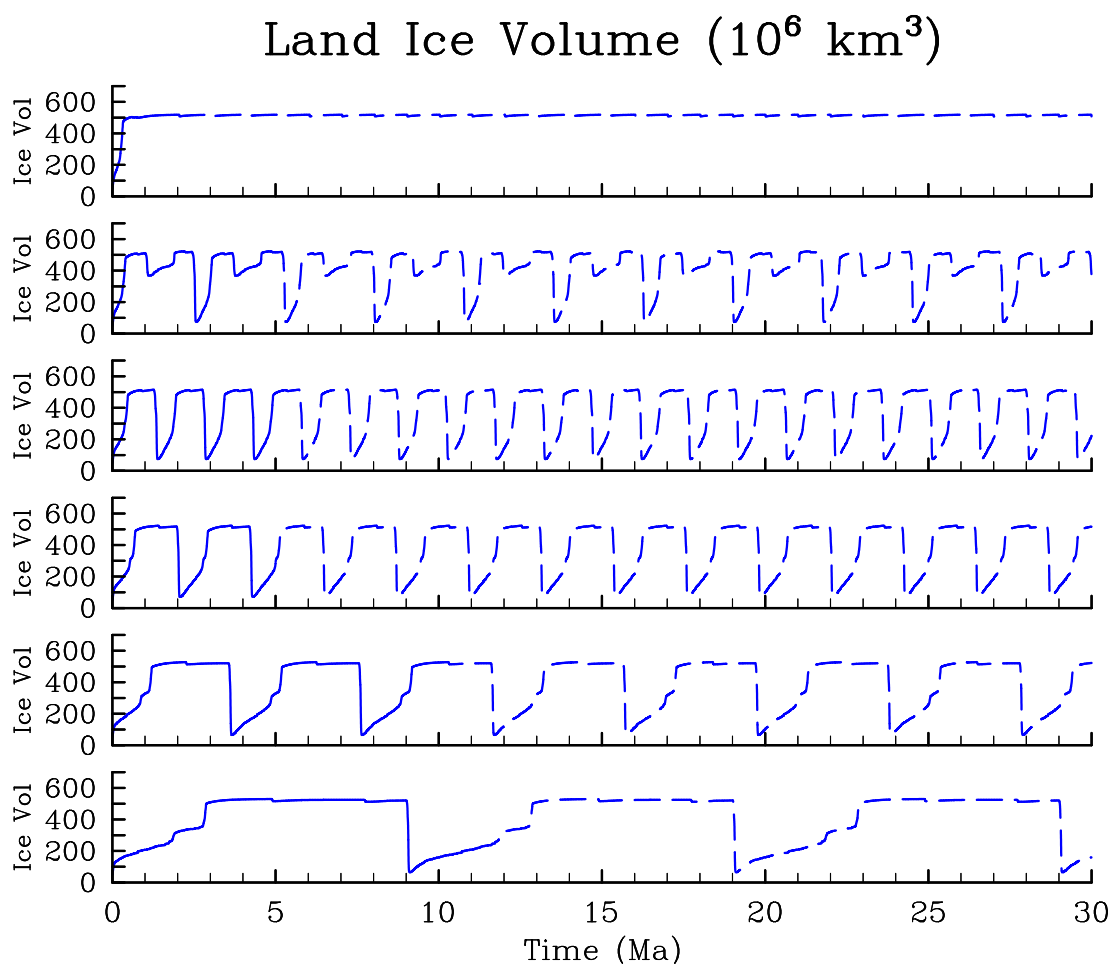
Land Ice Volume (10^6 km^3)

Figure S2 Similar to figure S1, but for the model based upon the assumption of a quadratic dependence (X=2) of pCO$_2$ on the mass of dissolved inorganic carbon in equation (2) of the text.
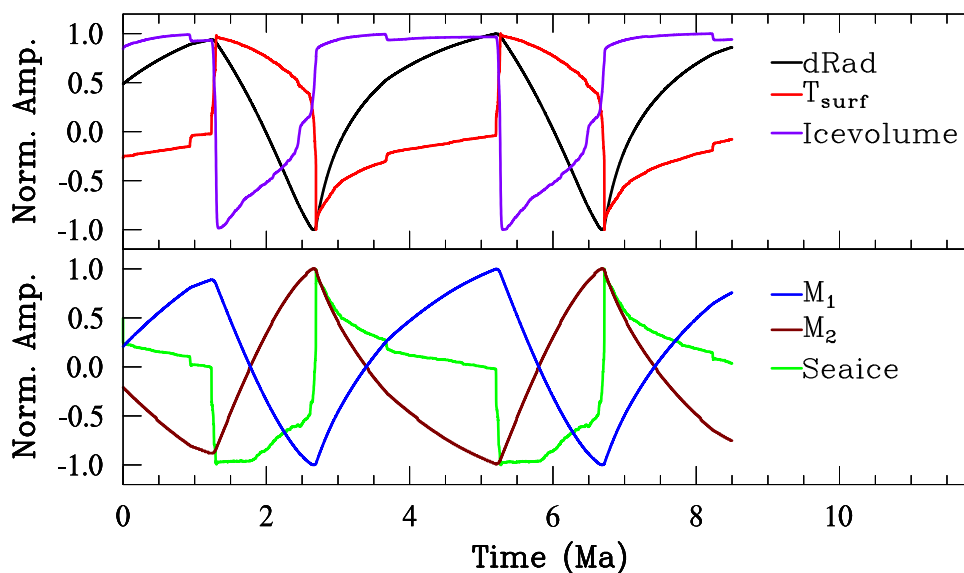
Figure S3 Amplitude normalized time series, with the mean removed, are shown for several ice age cycles and for 6 different field variables of the model. These include the variation in the infrared radiative forcing at the surface of the Earth, the mean surface temperature, land ice volume, the masses of the inorganic and organic carbon reservoirs and sea ice area.
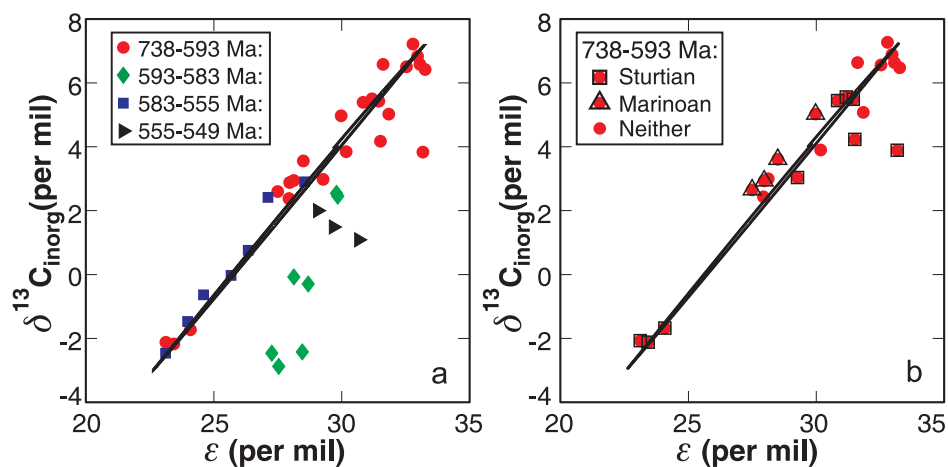
Figure S4 This representation of the dependence of $\delta^{13}C_{inorg}$ upon ε is similar to figure 6 in the main body of the paper except that this is for the model with the control parameter "*X*" set equal to 1.

factors in *V. cholerae*. But this idea raises possible public-health issues: the activation of quorum sensing in *V. cholerae* also induces active movement of the bacterium, potentially mobilizing the pathogen and encouraging the spread of infection from one person to another.

For several years, the repertoire of bacterial quorum-sensing signal molecules and receptors was thought to be rather limited and restricted to a few species. But recent studies have revealed an array of different signals, suggesting that we have only just scratched the surface of possible mechanisms. As new signals are identified and their use by bacteria is assessed, the list of quorum-sensing organisms will undoubtedly grow. We may eventually reach a point at which bacteria that do not engage in quorum sensing are regarded as the exception, rather than the norm. The challenge now is not only to identify new systems, but also to make sense of why an organism would use one type of system over another. ■

Matthew R. Parsek is in the Department of Microbiology, University of Washington, Box 357242, Seattle, Washington 98195-7242, USA.
e-mail: parsem@u.washington.edu

1. Miller, M. B., Skorupski, K., Lenz, D. H., Taylor, R. K. & Bassler, B. L. *Cell* **110**, 303–314 (2002).
2. Zhu, J. *et al. Proc. Natl Acad. Sci. USA* **99**, 3129–3134 (2002).
3. Camilli, A. & Bassler, B. L. *Science* **311**, 1113–1116 (2006).
4. Higgins, D. A. *et al. Nature* **450**, 883–886 (2007).
5. Sperandio, V. *Expert Rev. Anti-infect. Ther.* **5**, 271–276 (2007).

PALAEOCLIMATE

Slush find

Alan J. Kaufman

A coupled model of palaeoclimate and carbon cycling turns up the heat on the idea that Earth once became a giant snowball. It supports instead a milder 'slushball Earth' history — but piquant questions remain.

Sediments laid down in the oceans during the late Neoproterozoic era, between about 850 million and 542 million years ago, tell a dramatic story. They contain wildly varying abundances of the carbon isotope ^{12}C, which is typically incorporated into organic matter during photosynthesis. The pattern of excess ^{12}C in carbonates immediately above and below glacial deposits seems to indicate that photosynthesis on Earth came to a halt during a series of ice ages. These observations are a foundation of the 'snowball Earth' hypothesis[1,2]: that, just before the first appearance of animals, Earth's surface might have been repeatedly frozen over, even at tropical latitudes.

Not necessarily so, say Peltier *et al.* on page 813 of this issue[3]. They apply basic ideas about the solubility of gases to a coupled model of climate and carbon cycling[4] during the frigid late Neoproterozoic era. The results that emerge might explain the oscillatory carbon-isotope compositions of carbonates across the Neoproterozoic glacial cycles, without resorting to the hard-snowball model. Instead, they could lend support to a milder variation on the same theme — 'slushball Earth'.

The slushball and snowball models both predict ice sheets on continents near the Equator, but with markedly different extents of ice covering the oceans. In the snowball version, the frozen planet is completely blanketed, and reflects most of the Sun's warming rays back into space. Temperatures plummet and surface processes, including life, largely cease. Escape from the snowball state probably requires the build-up of volcanic carbon dioxide in the atmosphere over many millions of years,

resulting in torrential acid rain and the intense weathering of exposed rocks during the global thaw.

The slushball model[5], by contrast, predicts open glacial oceans that would have constrained runaway refrigeration by allowing sunlight to warm the planet's surface, driving an active hydrological cycle[6] and photosynthesis[7] in exposed seas. The end of such an ice age need not have required extreme amounts of CO_2 in the atmosphere, nor have been delayed for millions of years.

Peltier and colleagues' new dynamic model[3] shows how climate and atmospheric oxygen might have combined to prevent a runaway snowball Earth. As the oceans cool during ice ages, lower temperatures allow atmospheric gases such as oxygen to diffuse more readily into the deep sea, forcing the oxidation of abundant dissolved organic carbon, formed initially by photosynthesis in surface waters, to CO_2. Released back to the atmosphere by this oceanic 'respiratory' process, the excess CO_2 would warm the planet and thereby end the glacial epoch.

What is particularly interesting about this model is that climate drives the carbon cycle (and so determines the stable levels of atmospheric CO_2). In the most recent ice ages, as well as for earlier interpretations of Neoproterozoic carbon-isotope anomalies[8], the assumption has instead been the other way around. The crucial difference is that the Neoproterozoic carbon cycle was conceivably buffered by a marine pool of dissolved organic carbon that was orders of magnitude larger than that in present-day oceans[4].

A.J. KAUFMAN

Figure 1 | A soluble solution? The large (5–8-cm high) carbonate crystal fans (black to dark grey), which seem to grow out of the sea floor in this polished slab of a Neoproterozoic 'cap carbonate' from Brazil, suggest the presence of high concentrations of dissolved inorganic carbon in sea water after the ice ages, together with the rapid accumulation of sediments. These fans are draped by grey to white, fine-grained carbonates, which near the top become red, probably because they contain the iron-oxide mineral haematite (Fe_2O_3). The isotopic composition of such geological deposits is a focus of Peltier and colleagues' model interpretation[3] of Neoproterozoic climate and carbon cycling.

A pertinent criticism of Peltier and colleagues' mathematical model is the uncertainty in its input parameters, in particular the assumption that levels of atmospheric oxygen were similar to those of today (around 21%). Biological[9] and geochemical[10–12] evidence indicates that oxygen levels were low throughout most of the Neoproterozoic, with a significant rise in breathable air around 550 million years ago — about the time animals first appeared on the planet. In that case, it seems likely that pervasive oxygenation of the atmosphere and the hydrosphere, including the vast pool of dissolved organic carbon, occurred millions of years after the extensive ice sheets of the Neoproterozoic had melted away. This rise, known as the Wonoka anomaly after the locality in South Australia in whose rocks it was first observed, is recorded in 550-million-year-old carbonates worldwide that are spectacularly rich in ^{12}C.

The coupled model also does not address certain hallmark geological features of the Neoproterozoic glacial episodes. These include the unexpected appearance of iron-bearing sediments in the glacial deposits, as well as the enigmatic 'cap carbonates' that lie immediately above them (Fig. 1). The co-occurrence of iron-oxide cements and glacial sediments implies that levels of soluble iron increased during

OCEANOGRAPHY

Siberian salt in the cellar

The Lomonosov ridge, a mountain range under the Arctic Ocean, gained unusual notoriety in August, when a Russian submarine expedition planted a rust-proof titanium flag there to reinforce the country's Arctic territorial claims.

Now Brian Haley and colleagues report in *Nature Geoscience* that the ridge furnishes evidence of Russia's past influence on the region — at least, on its ocean circulation (B. A. Haley *et al. Nature Geosci.* doi:10.1038/ngeo.2007.5; 2007). They study neodymium (Nd) isotopic ratios in marine sediments in a core of sediments drilled from the Lomonosov ridge near the North Pole, at a sea depth of 1,250 metres.

The core represents a historical sketch of Arctic oceanography over the past 65 million years. The authors' big news is that the ratio $^{143}Nd/^{144}Nd$ of deep Arctic water that is preserved in the sediments was consistently far higher in the Neogene period between 15 million and 2 million years ago than it is now,

indicating the influence of young, mantle-derived rock. In the past 2 million years, similarly high ratios are found only during short ice ages.

Haley *et al.* argue that the only credible source for such a signal is material from the Putorana basalts of the Central Siberian Plateau. But how did a surface-water signal from the Siberian coastal shelf sink to the great depths of the Lomonosov ridge?

The authors see the answer in the wider global climate, and the opening up of the Fram Strait 17.5 million years ago. This strait is the only deep passage for water to and from the Arctic, and runs roughly along the Greenwich meridian between Greenland and the Norwegian island of Spitsbergen. Its breaching allowed warm, saline waters to flow into the Arctic from the Atlantic. As these waters entered colder climes, evaporation increased, causing more precipitation and the growth of extensive floating ice shelves at northerly latitudes —

SWEDISH POLAR RESEARCH SECRETARIAT

including along the Siberian coast.

As sea water freezes, it rejects salt. Haley *et al.* propose that the resulting denser, briny water that sank beneath the developing ice sheet carried Russian sediment to the Lomosonov ridge during the Neogene, as it similarly does off Antarctica today.

Waters from the North Atlantic drift have low neodymium ratios. The authors estimate that, to maintain the ratios of the Neogene core record after the initial influx following the Fram breach, the flow of warm water from the Atlantic into the Arctic could have been no more than half of that today. They suggest that the Atlantic conveyor belt must

at that time have stopped at a more southerly point than it does today. This is a well-established prediction for recent ice ages, which indeed also produce high neodymium ratios in the Arctic cores. But how it would have been maintained as an equilibrium state during the entire Neogene is unclear.

The model of an Arctic circulation dominated by seawater subduction off the Russian coast contrasts with today's picture, in which the Arctic is under a steady North Atlantic influence. In sketching the Arctic's sensitivity to past climate change, Haley *et al.* underscore its vulnerability to further change today.

Richard Webb

---

the ice age. As iron-bearing minerals such as haematite (Fe_2O_3) are remarkably insoluble in the presence of oxygen, large regions of the ocean must have been largely anoxic during the glacial periods — at odds with the authors' suggestion of progressive oxygenation. A whiff of oxygen would have caused an iron-rich sea to rust, potentially consuming much of the oxidant needed to convert dissolved organic carbon to CO_2. Other potential sinks for oxygen, including weathering of the continents and the oxidation of volcanic gases, were similarly overlooked in the model exercise.

The cap carbonates are testament to the extreme build-up of carbonate anions (alkalinity) in sea water during the Neoproterozoic glacial episodes, and to their wholesale accumulation as carbonate minerals in the glacial aftermath. The oxidative respiration of organic matter produces CO_2 and also creates alkalinity, so Peltier and colleagues' open-ocean solution might also explain the ubiquitous presence of the cap carbonates. But as the authors acknowledge[3], there are other possible oxidants that would work in an anoxic glacial ocean — sulphate, for example[13]. In the absence of free oxygen, sulphate-reducing bacteria could have occupied the water column, as they do in the Black Sea today, and could have fed on the standing pool of organic carbon, progressively raising the concentrations of inorganic carbon. At the same time, their metabolic activity would have released hydrogen sulphide

that, when combined with iron, would form the highly insoluble mineral pyrite (FeS_2). The resultant rain of pyrite to the sea floor might help to explain extreme sulphur-isotope variations that are notably present in the post-glacial cap carbonates[14].

These texturally and isotopically distinct carbonates figure prominently in Neoproterozoic palaeoclimate interpretations. In Peltier and colleagues' model, the ^{12}C-rich cap carbonates reflect one stable state of the carbon cycle. But notably, isotopically similar carbonates also accumulated immediately before the ice ages[7,15]. Depending on the timing of CO_2 release, the presence of these deposits can effectively neutralize the authors' proposed solubility hypothesis for the Neoproterozoic ice ages. Not only is more oxygen dissolved when the oceans get colder, so too is more CO_2, which makes water acidic. Acidification of the oceans would have a profound effect on the preservation of carbonate deposited before or after the ice ages.

The variable accumulation of carbonate and iron-oxide-rich deposits across the glacial cycles is not necessarily incompatible with Peltier and colleagues' slushball model[3]. It could well reflect regional differences in seawater salinity and pH, as well as levels of soluble oxygen, sulphate, iron and dissolved organic and inorganic carbon in sea water. The idea of a self-limiting climate as expressed in their model is a tantalizing prospect, and an

important contribution to the debate. But our poor understanding of Neoproterozoic ocean dynamics and oxidation add great uncertainty to such mathematical models of Neoproterozoic climate and carbon cycling. ■

Alan J. Kaufman is in the Geology Department, University of Maryland, USA, and is currently on sabbatical at the Geologisch–Paläontologisches Institut, Westfälische Wilhelms-Universität Münster, Corrensstraße 24, 48149 Münster, Germany.
e-mail: kaufman@geol.umd.edu

1. Kirschvink, J. L. in *The Proterozoic Biosphere: A Multidisciplinary Study* (eds Schopf, J. W. & Klein, C.) 51–52 (Cambridge Univ. Press, 1992).
2. Hoffman, P. F., Kaufman, A. J., Halverson, G. P. & Schrag, D. P. *Science* **281,** 1342–1346 (1998).
3. Peltier, W. R., Liu, Y. & Crowley, J. W. *Nature* **450,** 813–818 (2007).
4. Rothman, D. H., Hayes, J. M. & Summons, R. E. *Proc. Natl Acad. Sci. USA* **100,** 8124–8129 (2003).
5. Hyde, W. T., Crowley, T. J., Baum, S. K. & Peltier, W. R. *Nature* **405,** 425–429 (2000).
6. Arnaud, E. & Eyles, C. H. *Sedim. Geol.* **183,** 99–124 (2007).
7. Olcott, A. N. *et al. Science* **310,** 471–474 (2005).
8. Kaufman, A. J., Knoll, A. H. & Narbonne, G. M. *Proc. Natl Acad. Sci. USA* **94,** 6600–6605 (1997).
9. Knoll, A. H. & Carroll, S. B. *Science* **284,** 2129–2137 (1999).
10. Fike, D. A. *et al. Nature* **444,** 744–747 (2006).
11. Canfield, D. E., Poulton, S. W. & Narbonne, G. M. *Science* **315,** 92–95 (2007).
12. Kaufman, A. J., Corsetti, F. A. & Varni, M. A. *Chem. Geol.* **237,** 47–63 (2007).
13. Hayes, J. M. & Waldbauer, J. R. *Phil. Trans. R. Soc. Lond. B* **361,** 931–950 (2006).
14. Hurtgen, M. T., Halverson, G. P., Arthur, M. A. & Hoffman, P. F. *Earth Planet. Sci. Lett.* **245,** 551–570 (2006).
15. Halverson, G. P. *et al. Geochem. Geophys. Geosyst.* **3,** 10.1029/2001GC000244 (2002).